# The BEC-BCS Crossover

Part III Mathematics
Department of Applied Mathematics and Theoretical Physics
Cambridge University

Felix Barber
Essay setter: Prof. Ben Simons

# Contents

# Chapter 1

# Introduction

The Bose Einstein Condensate (BEC) was first predicted in a paper submitted to the renowned physicist Albert Einstein by the then inconspicuous Satyendra Nath Bose. Einstein was favourably impressed by the work, and translated the text from English to German for publication in the *Zeitschrift für Physik*. The paper was published in 1924 [1]. Fourteen years later in 1938 the phenomenon of Bose Einstein Condensation was first observed, in the transition from viscous liquid Helium I to the non-viscous liquid Helium II as documented by Kapitza, Allen and Misener [2]. BECs are a fascinating class of materials in their own right, with a wealth of literature devoted to their study. Within this essay we shall focus on the connection between BECs and the BCS superconducting state, so named after the theorists who initially proposed the theory in 1957: John Bardeen, Leon Neil Cooper and Robert Schrieffer [3].

When BCS theory was first proposed the BEC and BCS states quickly came to represent two distinct paradigms describing superfluidity and superconductivity within the regions of low temperature physics that had been explored at that point. BCS superconductors are fermionic systems which are reasonably modelled using an extremely weak attractive interaction between fermions of opposite spin with strength characterised by the coupling constant $g$ (these fermions can be, but are not required to be, electrons). This interaction leads to a pairing instability for electrons above the Fermi surface, as well as the resultant formation of the Cooper state of fermions. Cooper pairs may be viewed as pairing in reciprocal space rather than real space. In contrast a BEC is a macroscopic occupation of the lowest energy state (ground state) in a system of bosons (commonly these are composite bosons).

The dissociation temperature of these composites far exceeds the BEC critical temperature $T_c$, so that near $T_c$ they may be viewed as having no internal degrees of freedom. The differences between the two states are ostensibly quite profound, and after the initial proposal of BCS theory began to be emphasised more than their similarities. The crossover between BEC and BCS was first addressed in a mean field treatment by Eagles [4] in a work on superconductivity in doped semiconductors with low carrier densities (eg $SrTiO_3$), where the attractive interaction does not need to be small compared to the Fermi energy. In a seminal work by Leggett the crossover was later studied in the context of a dilute fermion gas [5]. Here Leggett described the extreme BCS and BEC states in the mean field approximation using the same form of ground state for each case, with a mind towards viewing liquid $^3$He condensation as the condensation of giant diatomic molecules. These works preceded the experimental realisation of the crossover by several decades, with experimental work in the early 2000s [6–8] prompting renewed interest in the subject.

We induce a crossover between the BCS and BEC states by decreasing the correlation length scale (roughly thought of as the size) of the cooper pairs relative to the average interparticle spacing. At a certain point this process causes the realisation of a bound molecular state; we then view the Cooper pairs as no longer being delocalised in real space and paired in reciprocal space, but rather as being a spatially localised molecule. In the limit of the correlation length of Cooper pairs becoming negligible relative to the average interparticle spacing, these molecular pairs are tightly bound enough to be accurately described as bosons exhibiting no internal degrees of freedom. The BEC state then corresponds to the condensation of this (now weakly repulsive) bosonic gas.

It is evident then that there are two methods by which one may drive the BCS to BEC crossover. One involves holding the interaction strength fixed and varying particle density, while the other entails fixing particle density and varying the interaction strength. Simply put, we hold one 'knob' fixed and tune the other. The two methods lend themselves to different realisations of the same physical phenomena: the former is more readily adopted within solid state physics (eg excitons) where the interactive potential is not easily adjusted and a two body bound state is always present, while the latter has seen extensive application within the field of ultracold atomic gases using an experimental technique known as a Feshbach resonance (see section 2.2). Within this essay we shall focus mainly on the realisation of this crossover

in ultracold atomic gases where the strength of the interactions may be easily tuned. Despite this, it should be noted that the problem is in fact far broader in scope, and may be realised in principle in essentially any fermionic system displaying a weak attractive interaction (such as, for example, neutron stars). Should the reader require further description of relevant literature, we direct them to [9] or a number of the other numerous reviews of ultra cold atomic physics [10–12].

The essay is structured as follows:

In chapter 2 we present the crossover viewed through the lens of the vacuum two-body scattering problem, introducing key results from scattering theory in the process. We follow this by introducing the Feshbach resonance.

In chapter 3 we discuss mean field theory approaches to the crossover within two different formulations to obtain physically intuitive results in the extreme BCS and BEC cases. The first uses manipulation of the BCS algebra, while the second relies on the path integral formulation.

In chapter 4 we briefly discuss the zero and finite temperature phase diagram in the population imbalance case.

In chapter 5 we review some experimental realisations of the crossover in both cold atomic gases and within Bose Einstein condensation of exciton polaritons.

Note to the reader: In the interest of brevity we neglect an explanation of the commonplace mathematical constructions adopted throughout this essay. For further reading we recommend texts on the theory of many body quantum systems [13, 14].

As a final note before beginning I would like to thank Ben Simons for first allowing this essay to take place, for taking time to talk me through numerous questions about the concepts involved, and for providing helpful encouragement throughout. In addition I would like to express my sincere gratitude to Marianne Bauer for providing fruitful conversations, advice and support when her own commitments were exceptionally demanding. Finally I would like to thank Martin Zwierlein, Wolfgang Ketterle and Mark Ku for kindly taking time to discuss their research with me in person.

# Chapter 2

# Scattering and the Feshbach Resonance

## 2.1 Scattering Review

Ultracold atomic vapours provide a concrete example of a physical system where the interactive strength between fermions may be varied at will. This has facilitated use of the BCS to BEC crossover with high levels of precision, finding applications within optical lattices as well as contributing to the observation of a range of interesting topological phenomena (discussed in chapter 5). Here we introduce the crossover as a scattering problem, introducing key results and phenomena associated with such.

In the two body scattering problem of finding the resultant wavefunction for a particle incident on some radial potential $V(r)$, we may always expand the wavefunction into an infinite sum of partial waves with coefficients characterised by phase shifts $\delta_l$ (here $l$ indexes the angular momentum of the partial wave). In the limit of low energy scattering the zero angular momentum ($l = 0$) $s$-wave scattering amplitude $f(k)$ dominates this expansion, characterising the scattered wavefunction [15].

$$f(k) = \frac{1}{k \cot\left(\delta_0(k)\right) - \mathrm{i}k} \tag{2.1}$$

This scattering amplitude depends upon the s-wave phase shift $\delta_0$, which may be conveniently

expressed in terms of the $s$-wave scattering length $a_s$:

$$\lim_{k\to 0} \delta_0 = -\tan^{-1}(ka_s). \tag{2.2}$$

Here $k$ corresponds to the incident momentum magnitude. We see that at low energies the $s$-wave scattering length to a good approximation characterises the vacuum two-body scattering problem. The low energy condition here is effectively a confinement of our consideration to low temperatures relative to the "centrifugal" potential barrier at finite angular momentum $l$ [9].

We now apply this knowledge of the vacuum scattering problem in a many body context. In the next section we shall describe a connection between $a_s$ and the strength of an interactive potential (often described as a "contact" potential using a Dirac delta function four-body term in the Hamiltonian with coupling constant $g$). In ultracold fermionic vapours this connection is exploited to induce a variation in the strength of the fermionic interaction simply by tuning the scattering length in a process known as a Feshbach resonance [6]. In the applications we consider this tuning is achieved by adjusting the strength of an applied magnetic field (our experimental 'knob').

In the case of low energy, $s$-wave (isotropic) scattering the Paul exclusion principle precludes the scattering of identical species of fermions [9], for the above process to work we must therefore consider a system comprising two populations of two distinct fermion species. These populations are for the most part assumed to be equal in size. The introduction of two species is effective in that it also addresses another concern: the insufficient thermalisation offered by $p$-wave elastic scattering collisions at low temperatures. By contrast to the single species case, introducing multiple species allows the low temperature regime to be accessed by normal evaporative cooling methods through thermalisation using $s$-wave scattering. The species considered may be different hyperfine states of the same atom, or two different elements altogether. For simplicity we consider the former case where these species have equal mass, however, the qualitative behaviour of the crossover should be similar in the event of small mass imbalances [10]. For simplicity we describe the hyperfine states here as "spin up" $|\uparrow\rangle$ and "spin down" $|\downarrow\rangle$.

## 2.2 Two-Channel Feshbach Resonance

In what follows the terms "open" and "closed" channels refer to two distinct states of the particles involved, which in this case of $^6$Li correspond to different spin states. Our two particles enter in what is known as the *open channel*. In $^6$Li (a system commonly used for experimental realisation of the crossover [17]) the electron spin is aligned in the same direction for each of the lowest hyperfine states, so that our particles necessarily enter in a spin triplet configuration. The *closed channel* contains a molecular bound state for two fermions arranged in the singlet configuration. This closed channel may couple to the states in the open channel by hyperfine interactions between electron and nuclear spin. A Feshbach resonance occurs when a quasibound molecular state in the closed channel couples resonantly with the open channel continuum of energy states. The two fermions are then temporarily trapped in this quasibound state for a lifetime which increases as the resonance is approached. One result of this resonance is an anomalously large scattering cross section $\sigma_{tot}$, given in the low energy approximation by

$$\sigma_{tot} = 4\pi a_s^2. \tag{2.3}$$

A divergence in scattering cross section is therefore associated with a divergence in $s$-wave scattering length. The difference in magnetic moment between the bound molecular state and the open channel states allows us to tune across this resonance experimentally through the application of a magnetic field to adjust the energy difference between the different channel states. The open channel then has a scattering length which on a phenomenological level varies with $B$ as

$$a(B) = a_{bg}\left(1 - \frac{\Delta B}{B - B_0}\right). \tag{2.4}$$

Here $a_{bg}$ is the background scattering length in the absence of coupling to the bound state. Since in most experimental applications $\Delta B a_{bg} > 0$ [11] this generally implies that with increasing field strength the scattering length should vary from positive to negative. Thus in order to transition from the BEC state (positive scattering length) to the BCS state (negative scattering length) one should drive from low magnetic fields to high. In experimental setups this is generally the easiest method of approach as it avoids additional condensate loss from 3 body collisions associated with ramping the field up to above the resonance before gradually

winding it down [6].

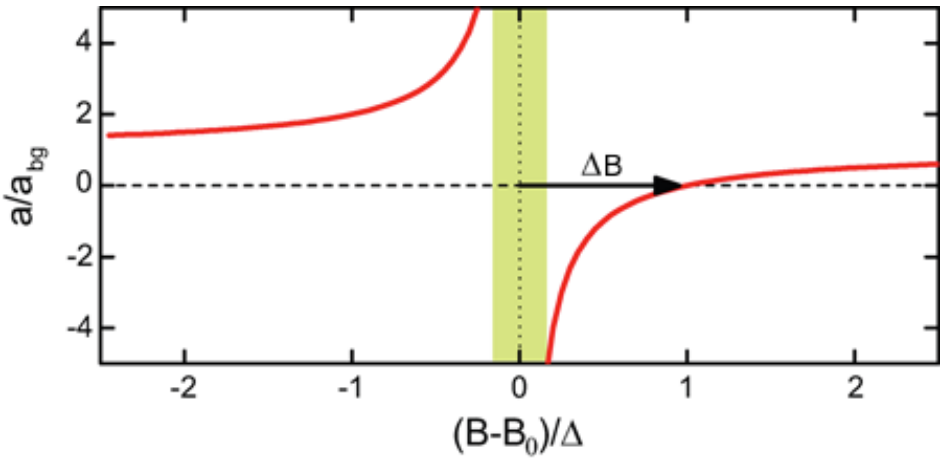


Figure 2.1: Plot of $s$-wave scattering length $a_s$ versus normalised magnetic field $(B-B_0)/\Delta B$ across a Feshbach Resonance (described mathematically by eq. 2.4). Figure taken from Ferlaino [16].

## 2.3 Single Channel Feshbach Resonance

It is often sufficient to describe the system using only a pseudopotential interaction between two single particle states of the form below, with scattering length given by eq. 2.5 [9].

$$V(\mathbf{r})(...) = \frac{4\pi\hbar^2 a_s}{2M_r}\delta(\mathbf{r})\frac{\partial}{\partial r}(r\ \ ...) \tag{2.5}$$

Here $M_r$ is the reduced mass of the pair. This form is of particular interest, sincethis pseudopotential also gives the form of scattering amplitude from equations 2.1 and 2.2, true below for arbitrary $k$. This result was noted initially by Fermi with slow neutrons, and Lee, Huang and Yang with weakly interacting quantum gases [9].

$$f(k) = -\frac{1}{1/a_s + \mathrm{i}k} \tag{2.6}$$

We now use this result to provide another perspective on the formation of a bound state when viewed alongside the two-channel model described above.

The scattering amplitude in eq. 2.6 has a simple pole at $k = \mathrm{i}K$ where $K = 1/a_s$. This pole lies in the upper half complex plane for $a > 0$. It is a general theorem [18] that poles of the scattering amplitude in the upper complex k plane are connected with bound states of binding energy $E_b = \hbar^2/(2M_r a_s^2)$.

As stated previously, by using the magnetic moment difference between this bound state and the single channel state we are able to tune the energy of this molecular state up to the zero energy continuum threshold. This corresponds to increasing the scattering length from a small positive value to a divergence to $\infty$ at resonance. We see from figure 2.1 and experimental findings [6] that as the energy of the molecular state is tuned above that of the incoming state the sign of $1/a_s$ changes, moving the pole in eq 2.6 to lie in the lower half $k$-plane, consistent with the fact that the molecular state is no longer truly bound. A full analysis of the direct effect on the scattering length of adjusting the detuning of the bound state from resonance in this manner is beyond the scope of this text, but produces a variation matching the phenomenological form in eq. 2.4 [9].

Another perspective using on the above is shown in the example of scattering from a square well attractive potential.

In the low energy scattering approximation the wavelengths of consideration are presumed to be far larger than the range of our interaction $r_o$. This simplification therefore still allows us to obtain insight as we expect results to be insensitive to the detailed potential structure. Solving the scattering problem for a free particle wavefunction incident on this square well potential one can see that with increasing potential well depth $V_o$ the scattering length diverges to $-\infty$ at the formation of a two body bound state of energy $E = 1/ma_s^2$ at the critical depth $V_o'$ (shown in fig. 2.2). Above this threshold the scattering length becomes positive, and may be interpreted as the size of the two-body bound state.

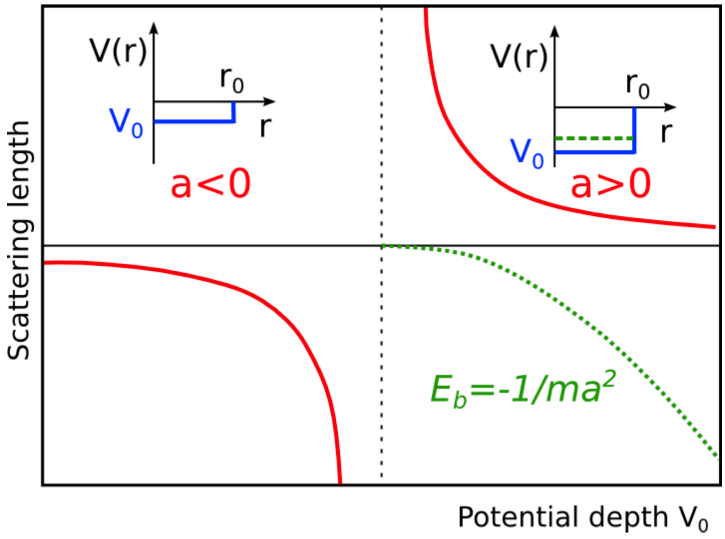


Figure 2.2: Plot of $s$-wave scattering length $a_s$ versus potential well depth $V_0$ for a finite square well potential. Insets show the formation of a two body bound state above the critical well depth. Figure taken from Randeria and Taylor [11]

## 2.4 Formalism

With an interaction strength $g$ this system may described by the following single-channel contact potential Hamiltonian [10]:

$$\hat{\mathrm{H}} - \mu\hat{\mathrm{N}} = \sum_{\mathbf{k}\,\sigma} (\epsilon_k - \mu)\, \hat{c}^\dagger_{\mathbf{k}\sigma}\hat{c}_{\mathbf{k}\sigma} - \frac{g}{L^d}\sum_{\mathbf{k}\,\mathbf{k}'\,\mathbf{q}} \hat{c}^\dagger_{\mathbf{k}\uparrow}\hat{c}^\dagger_{\mathbf{k}'\downarrow}\hat{c}_{\mathbf{k}'+\mathbf{q}\downarrow}\hat{c}_{\mathbf{k}-\mathbf{q}\uparrow}. \tag{2.7}$$

Here $g > 0$ represents the strength of an attractive contact interaction, $L^d$ the volume of the system (dimension $d$), and we assume a parabolic dispersion relation of form $\hbar^2k^2/2m$ (note, however, that for the coming sections we will set Planck's constant equal to 1).

It is interesting to note that in a renormalization group framework the coupling constant $g$ determining the strength of the interaction term in this Hamiltonian satisfies the RG equation [19]

$$\frac{\mathrm{d}g}{\mathrm{d}l} = (2-d)g - \frac{g^2}{2}. \tag{2.8}$$

We see that for $d > 2$ there is a repulsive fixed point at $2(2-d) < 0$, with weaker attractive

couplings flowing to zero (no bound state) and stronger attractive couplings flowing to $-\infty$ (bound state) [19]. We note also that at $d = 2$ this fixed point meets the trivial fixed point at $g = 0$, however, despite this and other interesting behaviours the specialised situation of $d = 2$ will not see further mention here.

To circumvent later pathologies arising from this contact interaction of eq. 2.7 the "bare" interaction strength $g$ is chosen such that it satisfies the following regularization condition:

$$\frac{m}{4\pi a_s} = -\frac{1}{g} + \sum_{\mathbf{k}} \frac{1}{2\epsilon_k}. \tag{2.9}$$

This relation may be derived by considering the Lippman-Schwinger equation applied to the above contact potential, as discussed by Randeria in the book by Griffin, Snoke and Stringari [20], and within [14]. We draw the reader's attention to the ultraviolet divergence in the energy summation - this is a false artefact of the contact potential. If the potential in 2.7 had a spatial extent characterised by $r_0$ then the summation would contain a cut-off at $\Lambda \approx 1/r_0$. The application of this Hamiltonian will be expanded upon further in chapter 3.

To close this section we briefly discuss the importance of length scales and their relation to the unitarity regime. In the absence of interactions the only length scale in the problem should be in the Fermi wavevector modulus $k_f$. However, we have seen that in the low energy limit all scattering properties may be expressed by means of the $s$-wave scattering length $a_s$. We therefore expect that in the low energy limit the dimensionless variable $1/k_f a_s$ should be sufficient to characterise the crossover dependencies of all physical observables associated with the system [5]. In this case the BEC and BCS regimes correspond to $1/k_f a_s \to \pm\infty$ respectively. We note that although the scattering length is seen to diverge in the unitarity limit, this does not lead to discontinuities in observable characteristics of the system as for a dilute gas the scattering length only appears in the form $1/k_f a_s$ which is continuous throughout. The threshold of bound state formation is known as the unitarity regime, and is the most strongly interacting regime in the entire crossover; in the $1/a_s \to 0$ limit the scattering amplitude has no length scale throughout.

# Chapter 3

In this section we explore multiple mean field theory (MFT) approaches to the BCS to BEC crossover. First we shall obtain a physically clear picture for our description of the BEC-BCS crossover as a crossover rather than a phase transition, through the two limits being described by the same form of MFT ground state wavefunction. After this we shall dive into analysing the BCS algebra in the BEC limit of strong interactions, and find that the gap equation effectively simplifies the two-body bound state Schrödinger equation. This method will produce physically intuitive results for the chemical potential $\mu$ and superconducting gap function $\Delta$ (otherwise known as the condensate order parameter) in this limit. The works references have used methods based on that developed by Leggett for zero temperature [Leggett]. We shall then see a more general derivation of similar results at finite temperature by employing the path integral formulation in the footsteps of Sa de Melo et al. [21]. These comparatively simple methods allow us to extract physically meaningful results for the chemical potential, condensate order parameter and critical temperature in the two limiting cases, but ultimately both fail in the intermediate regime (particularly in the region of unitarity at $1/k_f a_s = 0$). Finally we shall introduce the zero temperature phase diagram as discussed by Parish *et al* [22].

## 3.1 BCS Algebra

We begin loosely following the work of Nozières and Schmitt-Rink [23], along with that of Parish [10] to illustrate the identical mean field ground state wavefunctions of the two states of matter. This work was assisted by Henly's notes on many body physics [24].

An approximate Hamiltonian for the two-component Fermi gas system was given in eq. 2.7. For sufficiently large $g$ two fermions form a bound pair in a spin singlet formation [23], with creation operator given by

$$\hat{b}^{\dagger}_{\mathbf{q}} = \sum_{\mathbf{k}} \phi_{\mathbf{k}} \hat{c}^{\dagger}_{\mathbf{k}\uparrow} \hat{c}^{\dagger}_{\mathbf{q}-\mathbf{k}\downarrow}. \tag{3.1}$$

The energy of this bound state is $-\epsilon_o + q^2/2M$ where $M = 2m$ is the total mass. Here $\phi_{\mathbf{k}}$ is the internal wave function, with characteristic spatial extent equal to $\epsilon_o^{-\frac{1}{2}}$. Recalling the form of the pairing energy for a bound state in a square well potential this illuminates our statement earlier that in the BEC limit of molecular pair formation the positive scattering length $a_s$ is roughly the size of the bound state. In the BEC limit (low densities, $1/k_f a_s \gg 1$) the ground state of this system of molecular pairs is then expected to be of the following form:

$$|\psi\rangle = N \exp\left[\lambda \sum_{\mathbf{k}} \phi_{\mathbf{k}} \hat{c}^{\dagger}_{\mathbf{k}\uparrow} \hat{c}^{\dagger}_{\mathbf{q}-\mathbf{k}\downarrow}\right]. \tag{3.2}$$

Where $\lambda = \langle b_0 \rangle$ is the condensate order parameter (recall that we are in the BEC regime with all fermions contained in molecular pairs), and $N$ is a normalization constant. Note that this bound state has the form of a coherent state for $k$-space pairs. Recall that in the non-particle conserving case the mean field BCS ground state has the form

$$|\psi\rangle = \prod_{\mathbf{k}} \left(u_{\mathbf{k}} + v_{\mathbf{k}} \hat{c}^{\dagger}_{\mathbf{k}\uparrow} \hat{c}^{\dagger}_{-\mathbf{k}\downarrow}\right) |0\rangle. \tag{3.3}$$

Here $u_{\mathbf{k}}$ and $v_{\mathbf{k}}$ are parameters which may be introduced through performing a standard Bogoliubov transformation on the Hamiltonian of eq. 2.7, where their values are fixed by requiring that the resultant Hamiltonian be diagonalised. Equivalently values of these parameters may be found by a variational method which assumes the form of the ground state in eq. 3.3, and then minimises the zero temperature expectation value for the free energy with respect to $v_{\mathbf{k}}$. We note that the parameters satisfy the normalization condition

$$|u_{\mathbf{k}}|^2 + |v_{\mathbf{k}}|^2 = 1, \tag{3.4}$$

while $v_{\mathbf{k}}$ has particular significance as the occupancy of the kth fermion state:

$$n_{\mathbf{k}} = \sum_{\sigma} \langle \psi | \hat{c}^{\dagger}_{\mathbf{k}\sigma} \hat{c}_{\mathbf{k}\sigma} | \psi \rangle = 2|v_{\mathbf{k}}|^2. \tag{3.5}$$

Note that in the case of $s$-wave pairing these parameters $u_{\mathbf{k}}$ and $v_{\mathbf{k}}$ can (and later will) be taken to be both real and functions only of the magnitude $k$ [10]. In fact, provided we assume $u_{\mathbf{k}}$ to be real, it is a simple task to prove that both $v_{\mathbf{k}}$ and $\Delta$ are real. We see that if we expand eq. 3.2 we reproduce the mean field theory BCS ground state of eq. 3.3 subject to

$$\frac{v_{\mathbf{k}}}{u_{\mathbf{k}}} = \lambda\phi_{\mathbf{k}}, \tag{3.6a}$$

$$N = \prod_{\mathbf{k}} u_{\mathbf{k}}. \tag{3.6b}$$

One may see this by observing that in a power series expansion of eq. 3.2 the product of any two fermionic creation operators for the same quantum state will yield zero. This leads to the annihilation of terms within the expansion as we move to higher order powers of the exponent. The fact that these two states of matter may be described by the same form of ground state can be used to provide a heuristic argument that they are indeed connected by a smooth crossover rather than a phase transition [23]. One intuitively imagines the parameters $u_{\mathbf{k}}$ and $v_{\mathbf{k}}$ varying continuously as the particle density or interactions are tuned between the two extremes. In a $p$-wave system (not discussed here) this is not the case, and there is indeed a phase transition between the BCS and BEC regimes [10].

In the limit $1/k_f a_s \to -\infty$ of the BCS regime the system represents an ideal non-interacting Fermi gas, resulting in $v_k = \Theta(\epsilon_k - \mu)$ and a filled Fermi sea. In a numerical evaluation at large but finite $1/k_f a_s$ this step function is smoothed out slightly by the pairing instability, though in this regime only a small minority of fermions within a limited range of the Fermi surface are unstable with respect to this pairing. In the limit of large $1/k_f a_s$ we see that the Fermi surface has been entirely lost.

Having shown that the ground states share a similar form, we now move on to a minimisation of free energy approach to the crossover, following closely the method taken by Parish [Parish]. Taking the zero temperature free energy operator $\hat{H} - \mu\hat{N}$ with contact interactive potential as given by eq. 2.7 we obtain two terms for the zero temperature expectation value $\mathrm{F} = \mathrm{E}_0 + \mathrm{E}_{\mathrm{pair}}$:

$$\mathrm{E}_0 = 2\sum_{\mathbf{k}} (\epsilon_k - \mu)|v_{\mathbf{k}}|^2, \tag{3.7a}$$

$$\mathrm{E}_{\mathrm{pair}} = -\frac{g}{L^d}\sum_{\mathbf{k}\,\mathbf{k}'} v_{\mathbf{k}}^* u_{\mathbf{k}} v_{\mathbf{k}'} u_{\mathbf{k}'} - \frac{g}{L^d}\sum_{\mathbf{k}\,\mathbf{k}'} |v_{\mathbf{k}}|^2 |v_{\mathbf{k}'}|^2. \tag{3.7b}$$

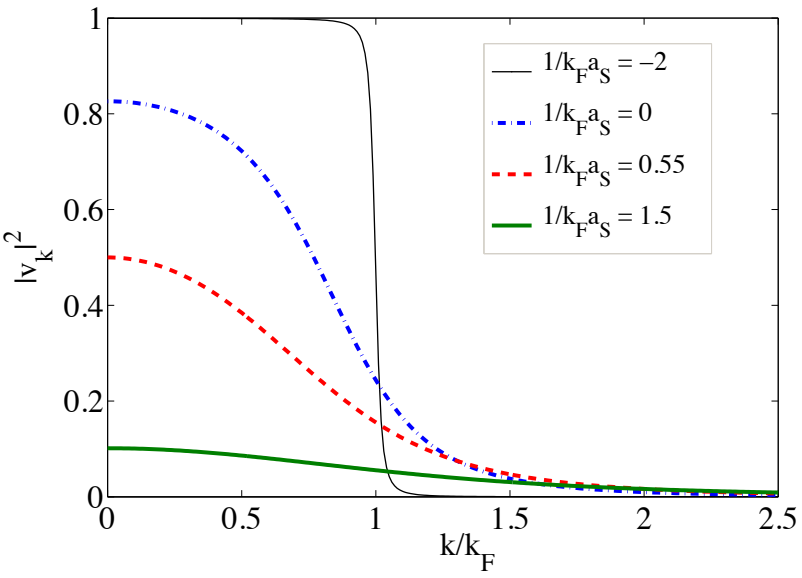


Figure 3.1: Plot of variation of the momentum distribution $|v_k|^2$ versus $k$ for various values of $1/k_f a_s$. Figure taken from Parish [10].

We can see this result through insertion of the BCS ground state, and as such will only provide a brief justification here. The term in eq. 3.7a simply arises from the single particle energy component of eq. 2.7, since we have already noted (without derivation, though the proof is trivial) that the expectation value $\langle n_{\mathbf{k}\sigma} \rangle = |v_{\mathbf{k}}|^2$, while the 2 originates from summation over spin.

In general the only way non-zero terms may be produced is if the creation/annihilation operators in eq. 3.8 below are paired with the annihilation/creation operator for the same state. The expectation of the pairing interaction of eq. 2.7 (re-written explicitly in eq. 3.8) therefore gives rise to non-zero terms in two separate instances, the results of which are shown above in eq. 3.7b.

$$\mathrm{E_{pair}} = -\frac{g}{L^d} \sum_{\mathbf{k}\,\mathbf{k}'\,\mathbf{q}} \langle 0 | \prod_{\mathbf{l}'} \left( u_{\mathbf{l}'} + v^*_{\mathbf{l}'} \hat{c}_{-\mathbf{l}'\downarrow} \hat{c}_{\mathbf{l}'\uparrow} \right) \hat{c}^\dagger_{\mathbf{k}\uparrow} \hat{c}^\dagger_{\mathbf{k}'\downarrow} \hat{c}_{\mathbf{k}'+\mathbf{q}\downarrow} \hat{c}_{\mathbf{k}-\mathbf{q}\uparrow} \prod_{\mathbf{l}} \left( u_{\mathbf{l}} + v_{\mathbf{l}} \hat{c}^\dagger_{\mathbf{l}\uparrow} \hat{c}^\dagger_{-\mathbf{l}\downarrow} \right) | 0 \rangle \quad (3.8)$$

The first term of eq. 3.7b comes from the $\mathbf{q} = \mathbf{0}$ terms within this expectation value. Considering $\mathbf{q} = \mathbf{0}$ eq. 3.8 reduces to

$$-\frac{g}{L^d} \sum_{\mathbf{k}\,\mathbf{k}'} \langle 0 | \left( v^*_{\mathbf{k}} \hat{c}_{-\mathbf{k}\downarrow} \right) \left( -v_{-\mathbf{k}'} \hat{c}_{-\mathbf{k}'\uparrow} \right) \left( -v_{-\mathbf{k}'} \hat{c}^\dagger_{-\mathbf{k}'\uparrow} \right) \left( v_{\mathbf{k}} \hat{c}^\dagger_{-\mathbf{k}\downarrow} \right) | 0 \rangle \quad (3.9)$$

where all other terms have vanished due to the normalisation condition eq. 3.4. Physically this simply corresponds to the particles scattering back into their initial states.

The second term of eq. 3.7b comes from taking $\mathbf{k} = -\mathbf{k}'$ in eq. 3.8. Relabelling and brief algebra yields

$$-\frac{g}{L^d}\sum_{\mathbf{k}\,\mathbf{k}'}\langle 0|\left(u^*_{\mathbf{k}'}+v^*_{\mathbf{k}'}\hat{c}_{-\mathbf{k}'\downarrow}\hat{c}_{\mathbf{k}'\uparrow}\right)v^*_{\mathbf{k}}\left(u_{\mathbf{k}}+v_{\mathbf{k}}\hat{c}^\dagger_{\mathbf{k}\uparrow}\hat{c}^\dagger_{-\mathbf{k}\downarrow}\right)v_{\mathbf{k}'}\,|0\rangle \tag{3.10}$$

In making the final step from eq. 3.10 to eq. 3.7b we make the assumption that (in the new labelling system) $\mathbf{k}' \neq \mathbf{k}$. In the original system this corresponds to $q \neq 0$, which has already been accounted for in the first term of eq. 3.7b.

Having justified the form of the two non-zero free energy terms given in eqs. 3.7a and 3.7b we follow Parish in minimising with respect to $v_k$ at constant chemical potential, producing equation 3.11.

$$2\left(\epsilon_k-\mu\right)u_{\mathbf{k}}v_{\mathbf{k}}-\left(u^2_{\mathbf{k}}-v^2_{\mathbf{k}}\right)\frac{g}{L^d}\sum_{\mathbf{k}'}u_{\mathbf{k}'}v_{\mathbf{k}'}=0 \tag{3.11}$$

Similar to Nozières and Schmitt-Rink, Parish notes that in the BEC limit $v_{\mathbf{k}} \ll 1$, leading to (in first order) the approximate form

$$2\left(\epsilon_k-\mu\right)v_{\mathbf{k}}-\frac{g}{L^d}\sum_{\mathbf{k}'}v_{\mathbf{k}'}=0 \tag{3.12}$$

Recalling $\epsilon_k = k^2/2m$ and taking $M = m/2$ to be the reduced mass this equation is nothing more than the Fourier transform of the two-body Schrödinger equation, with wavefunction given to first order by $v_{\mathbf{k}} = \lambda\phi_{\mathbf{k}}$ and where the chemical potential is filling the energy eigenvalue role. We see that in the BEC limit we recover the formation of bound pairs with wavefunction $\phi_{\mathbf{k}}$ and chemical potential $\mu = -E_b/2$ (the factor of a half here corresponds to the fact that two particles combine to form the molecular bound state).

In the general case of a $k$-dependent potential $V_{\mathbf{k}\,\mathbf{k}'}$ we obtain the BCS algebra (gap equation and density equation) given below in equations 3.13 and 3.14). The BCS algebra holds at any interaction strength, however, the interpretation and values of the order parameter delta may be seen to vary significantly as we move across the crossover.

$$\Delta_{\mathbf{k}}=\frac{1}{L^d}\sum_{\mathbf{k}'}V_{\mathbf{k}\,\mathbf{k}'}\frac{\Delta_{\mathbf{k}'}}{2E_{\mathbf{k}'}} \tag{3.13}$$

$$n_{\mathbf{k}} = \frac{1}{2}\left[1 - \frac{\epsilon_{\mathbf{k}} - \mu}{E_{\mathbf{k}}}\right] \tag{3.14}$$

Here $E_{\mathbf{k}}$ is given in eq. 3.15 and $\xi_k = \epsilon_k - \mu$. In the low energy limit the $k$-dependence of the SC gap may be neglected, simplifying eq. 3.13 to an equation in only one variable. Noting that in the BEC limit $v_{\mathbf{k}} \approx \Delta/(2E_{\mathbf{k}}+E_b)$, Parish observes that the density equation $n = \sum_{\mathbf{k}} v_k^2/L^d$ may be used to fix $\Delta$, with the finding that in this limit $\Delta = E_F/\sqrt{k_f a_s} = \sqrt{2E_f E_b}$. In this limit we no longer interpret $\Delta$ as the quasiparticle spectral gap from conventional BCS theory, but rather as a normalisation constant for the two-body wavefunction. One reason for this shift is that for a negative chemical potential the minimum quasiparticle energy is no longer delta, but instead becomes $\sqrt{\mu^2 + \Delta^2}$. This may be readily seen from the form of the quasiparticle dispersion relation in eq. 3.15.

$$E_{\mathbf{k}} = \sqrt{(\epsilon_k - \mu)^2 + \Delta_{\mathbf{k}}^2} = \sqrt{\xi_k^2 + \Delta_{\mathbf{k}}^2} \tag{3.15}$$

The result referred to here by Parish was observed by Randeria *et al.* [25]. The authors' method involved taking the low energy limit of the scattering $\hat{T}$ matrix from the Born series, obtaining in the low density limit simultaneous equations in $\Delta$ and $\mu$.

At this point we have shown that in the BEC limit both the chemical potential and superconducting gap yield physically insightful results. In the BCS regime the algebra above yields the standard BCS results for chemical potential $\mu = E_f$ and exponentially decaying superconducting gap $\Delta \propto \exp[-\pi/2k_f|a|]$, with a cooper pairing instability present at arbitrarily small strengths of attraction.

## 3.2 Field Theoretic Approach

Having introduced the physically intuitive work above in the $T = 0$ case, we now proceed to discuss a field theoretic MFT approach to obtaining similar results in the finite temperature case. We follow from Sa de Melo et al. [21], drawing on help from texts on the subject [14,20].

Our first goal is to obtain the saddle point approximation condition for the quantum partition function, shown in eq. 3.16 for the specific Hamiltonian of eq. 2.7 (recast here using

anticommuting Grassmann fields). We are considering the system at temperature $\beta = 1/T$.

$$\mathcal{Z} = \int\limits_{\substack{\overline{\psi}(\beta)=\xi\overline{\psi}(0)\\ \psi(\beta)=\xi\psi(0)}} \mathcal{D}\left[\overline{\psi},\psi\right] e^{-\mathcal{S}\left[\overline{\psi},\psi\right]} \tag{3.16a}$$

$$\mathcal{S}\left[\overline{\psi},\psi\right] = \int_0^\beta \mathrm{d}\tau \left[\sum_{\mathbf{k}\,\sigma} \overline{\psi}_{\mathbf{k}\sigma}\left(\partial_\tau + \xi_k\right)\psi_{\mathbf{k}\sigma} - gL^3 \int \mathrm{d}^3 r \overline{\psi}_\uparrow\left(\underline{r}\right)\overline{\psi}_\downarrow\left(\underline{r}\right)\psi_\downarrow\left(\underline{r}\right)\psi_\uparrow\left(\underline{r}\right)\right] \tag{3.16b}$$

We introduce the Hubbard-Stratonovich decoupling using the complex commuting field $\Delta$ to obtain the following (here we introduce the notation $\int \mathrm{d}x = \int_0^\beta \mathrm{d}\tau \int \mathrm{d}^3 r$):

$$\begin{aligned}\mathcal{Z} = \int \mathcal{D}\left[\overline{\Delta},\Delta\right]\mathcal{D}\left[\overline{\psi},\psi\right] \\ \times \exp\left[-\int \mathrm{d}x \left(\frac{|\Delta(r,\tau)|^2}{gL^3} + \overline{\Delta}\psi_\downarrow\psi_\uparrow + \Delta\overline{\psi}_\uparrow\overline{\psi}_\downarrow\right) - \int \mathrm{d}\tau \sum_{\mathbf{k}\,\sigma} \overline{\psi}_{\mathbf{k}\sigma}\left(\partial_\tau + \xi_k\right)\psi_{\mathbf{k}\sigma}\right].\end{aligned} \tag{3.17}$$

Eliminating the Grassmann fields $\psi$ by use of Gaussian integration we reach the form

$$\mathcal{Z}\int \mathcal{D}\left[\overline{\Delta},\Delta\right]\exp\left[-\int \mathrm{d}x \frac{|\Delta|^2}{gL^3} + \mathrm{Tr}\ln\hat{\mathscr{G}}^{-1}\right]. \tag{3.18}$$

where we have introduced the so-called *Gorkov Hamiltonian* $\hat{\mathscr{G}}^{-1}$ as

$$\hat{\mathscr{G}}^{-1} = \begin{pmatrix} \partial_\tau - \frac{\partial^2}{2m} - \mu & \Delta \\ \overline{\Delta} & \partial_\tau + \frac{\partial^2}{2m} + \mu \end{pmatrix}. \tag{3.19}$$

We introduce Matsubara frequencies $\omega_n$, and vary the action with respect to $\overline{\Delta}$. At this stage we also make the simplifying assumption that that the order parameter ext remising the action be constant in both space and time. Finally we obtain the stationary point condition for the action as

$$\frac{\Delta}{g} = \frac{1}{\beta L^d}\sum_{\mathbf{k}\,\omega)\mathbf{n}} \frac{\Delta}{\omega_n^2 + \xi_k^2 + |\Delta|^2} \tag{3.20}$$

This equation is essentially a reproduction of the BCS gap eq. 3.13. We now use the Matsubara frequency summation method described in the book by Altland and Simons [14] to obtain the following equation for critical temperature (noting that at $T_c$ we have $\Delta = 0$).

$$\frac{1}{g} = \sum_{\mathbf{k}} \frac{\tanh\left(\xi_k/2T_c\right)}{2\xi_k} \tag{3.21}$$

The apparent ultraviolet divergence in the summation above is a pathology of the contact potential used in eq. 2.7, and (as mentioned in chapter 2) is regularised by enforcing eq. 2.9

on the bare interaction $g$. As noted earlier, in the event that the potential used decayed on a length scale $r_0$ the summations in both eqs. 2.7 and 2.9 would have a (rough) cutoff at wavevector $\Lambda = 1/r_0$. Using this regularization condition we obtain

$$-\frac{m}{4\pi a_s} = \sum_{\mathbf{k}} \left[ \frac{\tanh\left(\xi_k/2T_c\right)}{2\xi_k} - \frac{1}{2\epsilon_k} \right]. \tag{3.22}$$

At this point one must use similar methods to obtain the number equation from the saddle point approximation to the Free energy:

$$\Omega_0 = \mathcal{S}_{\text{eff}}\left[\Delta = 0\right]/\beta. \tag{3.23}$$

Evaluating the number density by varying with respect to mu and applying an analogous procedure to that shown above we obtain

$$n = n_0(\mu, T) = \sum_{\mathbf{k}} \left( 1 - \tanh\left( \frac{\xi_k}{2T} \right) \right). \tag{3.24}$$

In the BEC and BCS extremes equations 3.22 and 3.24 may be solved to determine the chemical potential and critical temperature values within these limits. In the weak coupling BCS limit Sa de Melo *et al.* note that $\mu \gg T_c$ [21], leading to the result that $\mu \approx E_f$. This may then be inserted into eq. 3.22, where use of the identity

$$\int_0^\infty \mathrm{d}z z^{1/2} \left[ \frac{\tanh\left((z-1)/2t\right)}{2(z-1)} - \frac{1}{2z} \right] = \ln\left( \frac{8\gamma}{\pi e^2 t} \right) \tag{3.25}$$

immediately yields (with $\gamma = e^c$, $c =$ Euler's constant)

$$T_c = \frac{8\gamma}{\pi e^2} \epsilon_F \exp\left[ -\frac{\pi}{2k_F|a_s|} \right]. \tag{3.26}$$

We now treat the BEC regime of equations 3.22 and 3.24. In chapter 2 we discussed the formation of a two-body bound state. This bound state can be associated with the loss of a Fermi surface as the chemical potential changes sign from positive to negative. Making the assumption that $T_c \ll |\mu|$ (validated as we shall see in the final result) we see that the hyperbolic tangent function in eq. 3.22 tends towards 1 as its argument becomes very large. In this approximation we may use the following identity to that in the BEC limit the chemical potential tends towards half the bound state energy $-E_b/2$.

$$\int_0^\infty \mathrm{d}z z^{1/2} \left[ \frac{1}{2(z+1)} - \frac{1}{2z} \right] \tag{3.27}$$

Inserting this form into equation 2.26 and recalling the density of states expression for the number density

$$n = \int_0^{\epsilon_F} \nu(\epsilon)\mathrm{d} \tag{3.28}$$

we obtain the result

$$T_c \approx \frac{E_B}{2\ln\left(\frac{E_B}{E_F}\right)^{\frac{3}{2}}}. \tag{3.29}$$

Note that in the limit $1/k_f a_s \to \infty$ the numerator in this equation can be seen to diverge as $(1/k_f a_s)^2$ while the denominator can be seen to diverge only logarithmically. We thus expect that $T_c$ here should diverge in the BEC limit. This forces us to reconsider our physical interpretation of $T_c$, and is representative of a failure in the MFT analysis in this limit. In brief the reason for this is that MFT limits $\Delta = 0$ to a description of purely non-interacting fermions. However, a Ginzburg-Landau expansion of the action in $\Delta$ demonstrates that in the strong coupling limit the system is effectively described by a weakly interacting Bose gas. This incorporation of fluctuations in $\Delta$ about zero is equivalent to the diagrammatic approach undertaken by Nozières and Schmitt–Rink [23], who instead used a diagrammatic approach to address the variation of $T_c$ in the strong coupling regime.

This has profound physical implications on two levels: firstly it implies that the temperature $T_c$ calculated above should be taken not as the transition temperature at which the system establishes coherence, but instead as the temperature corresponding to pair breaking $T_{\mathrm{diss}}$. In the BCS limit these temperatures are the same and destruction of the condensate and pair breaking occur at the same scale, so the distinction is unnecessary. In the BEC limit this is not the case, and condensation occurs at a temperature $T_c$ significantly lower in scale than that of pair breaking $_{\mathrm{Tdiss}}$.

Secondly we see that in the BEC regime at temperatures significantly lower than that of pair dissociation the system above may be adequately described using the well understood theory of the weakly interacting Bose gas.

We conclude by remarking that the results obtained by Sa de Melo *et al.* [21] can clearly be seen to match those predicted in section 3.1 using conventional BCS theory, while extending their validity to the finite temperature regime. We should, however, note that although these results are physically interesting they do leave unanswered the question of how the system

properties vary in the intermediate regime $k_f a_s \geq 1$. This is considered further in the next chapter.

# Chapter 4

# Population Imbalance

In this section we briefly address the zero temperature and finite temperature phase diagrams, derived in the case of a population imbalance by Parish et al [22]

The population imbalance case is addressed in their method by adjusting the single channel Hamiltonian of eq. 2.7 to include different chemical potentials for the separate hyperfine states within a single atomic species as shown:

$$\hat{H} - \mu_{\uparrow}\hat{n}_{\uparrow} - \mu_{\downarrow}\hat{n}_{\downarrow} \tag{4.1}$$

This population imbalance can be imposed (for example) through the application of a Zeeman splitting magnetic field, leading to

$$\mu_{\uparrow} = \mu + h \qquad \mu_{\downarrow} = \mu - h \tag{4.2}$$

Using the MFT saddle point approximation for the free energy of eq. 3.23 Parish et al. obtain the following form for the mean-field free energy density:

$$\Omega^0 = -\frac{\Delta^2}{g} + \frac{1}{L^d}\sum_{\mathbf{k}}(\xi_k + E_{\mathbf{k}}) - \frac{1}{\beta L^d}\sum_{\mathbf{k}}\left(\ln\left(1 + e^{-\beta(E_{\mathbf{k}}-h)}\right) + \ln\left(1 + e^{-\beta(E_{\mathbf{k}}+h)}\right)\right) \tag{4.3}$$

Minimising this energy density with respect to the order parameter $\Delta$ and analysing the form of solutions is employed as a means to infer phase boundaries between different states. Determining the phase diagram through this mean field analysis is valid in the $T = 0$ regime,

and was employed successfully to demonstrate the existence of a quantum critical point when the transition from the superfluid state to the normal state changes from first to second order [22]. However, at finite temperature the MFT approximation to the free energy is insufficient as it fails to incorporate the contribution of non-condensed pairs to the density and magnetisation. As Parish et al. comment, in the region $\Delta = 0$ (this condition holds along the boundary of a second order phase transition) this contribution is effectively corrected for using the Nozières-Schmitt-Rink (NSR) term [23]:

$$\Omega^1|_{\Delta=0} = \frac{1}{\beta L^d} \sum_{\mathbf{q}\, \mathrm{i}\omega} \ln \Gamma^{-1}(\mathbf{q}, \mathrm{i}\omega) \tag{4.4}$$

where

$$\Gamma^{-1}(\mathbf{q}, \mathrm{i}\omega) = -\frac{1}{g} - \frac{1}{2L^d} \sum_{\mathbf{p}} \frac{\tanh\left[\frac{\beta}{2}(\xi_{\mathbf{p}} + h)\right] + \tanh\left[\frac{\beta}{2}(\xi_{\mathbf{p}+\mathbf{q}} - h)\right]}{\mathrm{i}\omega + \xi_{\mathbf{p}} + \xi_{\mathbf{p}+\mathbf{q}}} \tag{4.5}$$

Using the above correction Parish *et al.* obtain results for the phase diagram of the population imbalanced system as a function of temperature and of spin imbalance (measured through the Zeeman field $h$). The authors note the presence of a line of quantum tricritical points with increasing interaction strength connecting the first and second order phase boundaries. This line may be seen to terminate on the BEC side of resonance at zero temperature.

The work of Parish *et al.* is interesting as it demonstrates not only the added accuracy of the NSR correction to the free energy, but also the limitations of the single-channel model described in chapter 2. As noted by the authors, in the unitarity regime the magnetisation displays non-monotonic behaviour with h. This result is unphysical, indicating a breakdown of the correction term's validity in this regime. The resolution of this breakdown is to limit the application of the Nozières-Schmit-Rink correction to Feshbach resonances with a finite width, an example of which is provided in the two-channel model described in chapter 2. By incorporating a correction based on this two-channel model in the unitarity regime the authors are able to obtain the phase diagram for this system at $1/k_f a_s = 0$.

# Chapter 5

# Experimental Realisation

In the last two decades there have been significant experimental advances, giving rise to renewed interest in this problem. In this section we introduce some of these experimental realisations to illustrate some of the fascinating topological and dynamical constructions which have been observed.

The formation of BECs in ultracold atomic gases was first demonstrated in 1995 by Anderson *et al.* [26] in Rubidium 87 atoms, by Davis *et al.* [27] with sodium atoms, and by Bradley *et al.* [28] in Lithium. These observations were critical in facilitating much further work on such systems. In 1998 the first realisation of the Feshbach resonance was observed in an optically confined gas of sodium atoms. Moving across a resonance one sees a condensate loss due to enhanced inelastic collisions in the unitarity regime. The resonance was located in this work through performing magnetic field ramps of increasing size, then using time-of-flight imaging [6] to determine the size of the condensate following said ramp.

In the years following these works the Bose Einstein Condensation of ultracold gases has become commonplace, while the experimental tool provided in the Feshbach resonance has seen interesting application in the production of topological excitations within BECs. Recent work has resulted in the observation of solitons and solitonic vortices in fermionic superfluids of $^6$Li near a Feshbach resonance [29,30]. A perfectly stationary soliton corresponds to a zero in the condensate wavefunction as it changes sign from positive to negative. By contrast non-stationary solitons have a phase angle variation of pi-epsilon. Recalling the form of superfluid

velocity as the gradient of the phase angle we see that this corresponds to a non-zero flow profile localised near the soliton.

$$\mathbf{j}(\mathbf{r},\tau) \approx \frac{\rho_\mathbf{0}}{\mathbf{m}} \partial\phi(\mathbf{r},\tau) \tag{5.1}$$

The resultant condensate flow across the soliton is seen as an effective movement of the soliton in the opposite direction. In BECs the majority of bosons reside within the condensate, meaning that a stationary soliton corresponds to zero particle density. In the BCS case only a small fraction of the population are involved with pairing, so that the wavefunction reduction near a soliton only reduces a small fraction of the overall particle density in that localised region.

In an experimental context soliton phase imprinting is produced through application of a laser to the sample, introducing an additional optical potential $U$ which advances the wavefunction phase over time as $\Delta\phi = 2Ut/\hbar$. An optical mask then defines the boundary of this potential, and hence the point at which a phase difference (our soliton) forms.

Although the focus of this essay has been on cold atomic gas systems, it is at this point appropriate to briefly note an application of the theory discussed in this essay to condensed matter systems. For a general review we direct the reader towards Griffin *et al.* [20]. The concept of exciton condensation was initially considered by Keldysh and Kozlov [31], who showed that a low-density system of excitons may behave like a weakly interacting Bose gas and hence undergo condensation. Since in these systems the interactive strength may not be readily tuned, one resorts instead to varying the particle density. At high densities, the excitons dissociate into a two-component plasma. However, in this regime the attractive Coulomb interaction between electrons and holes can cause a instability with respect to a phase similar to that of BCS, an exciton insulator with a nonzero quasiparticle excitation gap present at the Fermi surface [14]. Polaritons are quasiparticle excitations produced by the coupling of a degenerate bosonic system to an external photon mode. The Bose Einstein condensation of exciton polaritons has been experimentally observed [8], with the bosonic system in question being one of quantum well excitons coupling to optical microcavities. Exciton plaritons have an extremely low mass in comparison to the atomic molecules discussed within this essay, and as such have the capacity to form undergo Bose Einstein condensation at large temperatures relative to the microKelvin regime of ultracold atomic gases. In this

study the polariton condensation was measured through characteristics such as coherence and population distribution, probed by analysis of their emission spectrum in the far field.

# Chapter 6

# Conclusion

We have presented the BCS to BEC crossover from multiple mean field theory standpoints. Factors which have been neglected include the bosonic gapless excitations within such systems - these may be modelled using fluctuations around the mean-field order parameter $\Delta$ [11]. We have also not presented any discussion of Quantum Monte-Carlo simulation, a numerical technique which has seen extensive application in the unitarity regime. Finally, no discussion has been posed towards the dynamical case of non-equilibrium driving across the Feshbach resonance, as studied by Barankov, Levitov and Spivak [32].

# Bibliography


[1] Bose, S. N. (1924). Plancks Gesetz und Lichtquantenhypothese. *Zeitschrift f'ur Physik*.

[2] Kapitza, P. (1938). Viscosity of liquid helium below the l-point. *Nature*, 26, 178–81,

[3] Bardeen, J., Cooper, L. N., Schrieffer, J. R. (1957). APS Theory of Superconductivity. *Physical Review*

[4] Eagles, D. M., (1969). APS Possible pairing without superconductivity at low carrier concentrations in bulk and thin-film superconducting semiconductors. *Physical Review*.

[5] Leggett, A. J. (1980). Diatomic molecules and Cooper pairs. *Modern trends in the theory of condensed matter*.

[6] Inouye, S., Andrews, M. R., Stenger, J., Miesner, H. J., Stamper-Kurn, D. M., Ketterle, W., (1998). Observation of Feshbach resonances in a Bose-Einstein condensate. *Nature*

[7] Regal, C. A., Greiner, M., & Jin, D. S. (2004). Observation of resonance condensation of fermionic atom pairs. *Physical review letters*, 92(4), 040403.

[8] Kasprzak, J., Richard, M., Kundermann, S., Baas, A., Jeambrun, P., Keeling, J. M. J., ... & Dang, L. S. (2006). Bos–Einstein condensation of exciton polaritons. *Nature*, 443(7110), 409-414.

[9] Bloch, I., Dalibard, J., & Zwerger, W. (2008). Many-body physics with ultracold gases. *Reviews of Modern Physics*, 80(3), 885.

[10] Parish, M. M. (2014). The BCS-BEC Crossover. *arXiv preprint* arXiv:1402.5171.

[11] Zwerger, W. (Ed.). (2011). *The BCS-BEC crossover and the unitary Fermi gas* (Vol. 836). Springer.

[12] Sheehy, D. E., & Radzihovsky, L. (2007). BEC–BCS crossover, phase transitions and phase separation in polarized resonantly-paired superfluids. *Annals of Physics*, 322(8), 1790-1924.

[13] Fetter, A. L., & Walecka, J. D. (2003). *Quantum theory of many-particle systems*. Courier Dover Publications.

[14] ÊAltland, A., & Simons, B. D. (2010). *Condensed matter field theory*. Cambridge University Press.

[15] Sakurai, J. J., & San Fu Tuan. (1994). *Modern quantum mechanics* (Vol. 104). Reading (Mass.): Addison-Wesley.

[16] Ferlaino, F., & Grimm, R. (2010). Forty years of Efimov physics: How a bizarre prediction turned into a hot topic. *Physics*, 3(9), 102.

[17] Moerdijk, A. J., Verhaar, B. J., & Axelsson, A. (1995). Resonances in ultracold collisions of Li 6, Li 7, and Na 23. *Physical Review A*, 51(6), 4852.

[18] Landau, L. D., & Lifschitz, E. M. (1987). *Mechanik*.

[19] Nikolić, P., & Sachdev, S. (2007). Renormalization-group fixed points, universal phase diagram, and 1/N expansion for quantum liquids with interactions near the unitarity limit. *Physical Review A*, 75(3), 033608.

[20] Griffin, A., Snoke, D. W., & Stringari, S. (Eds.). (1996). *Bose-Einstein Condensation*. Cambridge University Press.

[21] De Melo, C. S., Randeria, M., & Engelbrecht, J. R. (1993). Crossover from BCS to Bose superconductivity: Transition temperature and time-dependent Ginzburg-Landau theory. *Physical review letters*, 71(19), 3202.

[22] Parish, M. M., Marchetti, F. M., Lamacraft, A., & Simons, B. D. (2007). Finite-temperature phase diagram of a polarized Fermi condensate. *Nature Physics*, 3(2), 124-128.

[23] Nozières, P., & Schmitt-Rink, S. (1985). Bose condensation in an attractive fermion gas: From weak to strong coupling superconductivity. *Journal of Low Temperature Physics*, 59(3-4), 195-211.

[24] Henly, C. L. *BCS Theory.* Accessed 16/04/2014: http://people.ccmr.cornell.edu/ clh/Book-sample/7.3.pdf

[25] Randeria, M., Duan, J. M., &Shieh, L. Y. (1990). Superconductivity in a two-dimensional Fermi gas: Evolution from Cooper pairing to Bose condensation. *Physical Review B*, 41(1), 327.

[26] Anderson, M. H., Ensher, J. R., Matthews, M. R., Wieman, C. E., & Cornell, E. A. (1995). Observation of Bose-Einstein condensation in a dilute atomic vapor. *Science*, 269(5221), 198-201.

[27] Davis, K. B., Mewes, M. O., Andrews, M. V., Van Druten, N. J., Durfee, D. S., Kurn, D. M., & Ketterle, W. (1995). Bose-Einstein condensation in a gas of sodium atoms. *Physical Review Letters*, 75(22), 3969.

[28] Bradley, C. C., Sackett, C. A., Tollett, J. J., & Hulet, R. G. (1995). Evidence of Bose-Einstein condensation in an atomic gas with attractive interactions. *Physical Review Letters*, 75(9), 1687.

[29] Yefsah, T., Sommer, A. T., Ku, M. J., Cheuk, L. W., Ji, W., Bakr, W. S., & Zwierlein, M. W. (2013). Heavy solitons in a fermionic superfluid. *Nature*, 499(7459), 426-430.

[30] Ku, M. J., Ji, W., Mukherjee, B., Guardado-Sanchez, E., Cheuk, L. W., Yefsah, T., & Zwierlein, M. W. (2014). Motion of a Solitonic Vortex in the BEC-BCS Crossover. *arXiv preprint* arXiv:1402.7052.

[31] Keldysh, L. V., & Kozlov, A. N. (1968). Collective properties of excitons in semiconductors. *Sov. Phys. JETP*, 27, 521.

[32] Barankov, R. A., Levitov, L. S., & Spivak, B. Z. (2004). Collective Rabi oscillations and solitons in a time-dependent BCS pairing problem. *Physical review letters*, 93(16), 160401.